Arabian Journal of Chemistry (2017) **10**, 1153–1166

King Saud University

Arabian Journal of Chemistry

www.ksu.edu.sa
www.sciencedirect.com

ORIGINAL ARTICLE

Poly (acrylonitrile-co-methyl methacrylate) nanoparticles: I. Preparation and characterization

M.S. Mohy Eldin [a,*], M.R. Elaassar [a], A.A. Elzatahry [a,1], M.M.B. Al-Sabah [b]

[a] *Polymer Materials Research Department, Advanced Technology and New Materials Research Institute, City for Scientific Research and Technology Applications, New Borg El-Arab City 21934, Alexandria, Egypt*
[b] *Department of Chemistry, Faculty of Science, Al-Azhar University, Cairo, Egypt*

Received 17 June 2013; accepted 20 October 2014
Available online 25 November 2014

KEYWORDS

Nano-poly (acrylonitrile-co-methyl methacrylate);
Precipitation polymerization;
Particles size;
Copolymer composition;
TGA;
FT-IR;

Abstract This work concerns the preparation and characterization of poly (acrylonitrile-co-methyl methacrylate) Copolymer, P(AN-co-MMA), nano-particles using precipitation polymerization technique. Potassium per-sulfate redox initiation system was used to perform polymerization process in an alcoholic aqueous system. The impact of different polymerization conditions such as comonomer concentration and ratio, polymerization time, polymerization temperatures, initiator concentration and co-solvent composition on the polymerization yield and particle size was studied. Maximum polymerization yield, 70%, was obtained with MMA:AN (90%:10%) comonomer composition. Particle sizes ranging from 16 nm to 1483 nm were obtained and controlled by variation of polymerization conditions. The co-polymerization process was approved by FT-IR and TGA analysis. The copolymer composition was investigated by nitrogen content analysis. Copolymers with a progressive percentage of PAN show thermal stabilities close to PAN Homopolymer. SEM photographs prove spherical structure of the produced copolymers. The investigated system shows promising future in the preparation of nanoparticles from comonomers without using emulsifiers or dispersive agents.

1. Introduction

With high development in nanoscience, micro and nano-structured polymers have attracted high interest due to their unique properties, such as porous structure, and high surface. On the other hand, a wide range of applications using micro and nano-structured polymers have been recently reported in specific for medical (Thapa et al., 2003; Cho and Borgens, 2012), and industrial applications (Cheng et al., 2005; Yang et al., 2005). Many methods such as seeded suspension polymerization,

* Corresponding author. Tel./fax: +20 002 03 4593 414.
E-mail address: m.mohyeldin@mucsat.sci.eg (M.S. Mohy Eldin).
[1] Address: Department of Chemistry, Faculty of Science, King Saud University, Saudi Arabia.
Peer review under responsibility of King Saud University.

Production and hosting by Elsevier

http://dx.doi.org/10.1016/j.arabjc.2014.10.037
1878-5352

water based emulsion and precipitation polymerization have been used to fabricate micro and nano-structured polymers (Chaitidou et al., 2008). It has been reported that, monodispersed micro and nano nanoparticles could be produced using precipitation polymerizations without using any stabilizers or surfactant (Chaitidou et al., 2008; Downey et al., 1999). Synthesis of hybrid organic–inorganic nanocomposites and molecularly imprinted polymers is considered as main products using precipitation polymerization (Chaitidou et al., 2008; Ye et al., 1999; Wei et al., 2006). Polymers based on acrylonitrile can be prepared by polymerization of acrylonitrile or other unsaturated monomers bearing nitrile groups in the presence of comonomers such as acrylamide and a cross-linker, e.g. divinyl benzene or bisacrylamide (Ivanov and Yotova, 2002; Cao, 2006). In the same context, Boguslavsky et al. (2005) have reported the preparations of polyacrylonitrile nanoparticles using dispersion/emulsion polymerization method (Boguslavsky et al., 2005). On the other hand, Lee et al. (2009) have reported the synthesis of poly(AN-*co*-IA-*co*-MA) nanoparticle using acrylonitrile, itaconic acid, and methyl acrylate via aqueous dispersion polymerization using hydrophilic PVA in a water/N,N-dimethylformamide mixture media. Highly dispersed and uniform polyacrylonitrile microspheres have been prepared using soapless emulsion polymerization in water initiated by KPS (Guangzhi et al., 2011). In this paper we synthesized nano-poly (acrylonitrile-co-methyl methacrylate) particles with controllable size using a simple and cheap precipitation polymerization technique for the first time without any emulsifier or dispersive agents.

2. Materials and methods

2.1. Materials

Methyl methacrylate (MMA) was purchased from ACROS (USA), potassium persulfate ($K_2S_2O_8$) and acrylonitrile (AN) were obtained from Fluka (packed in Switzerland). Ethyl alcohol absolute was obtained from El-Nasr Pharmaceutical Co. for Chemicals (Egypt). Mixed indicator, Special for ammonium titration (Methyl Red + Methyl Blue dissolve in Ethanol), was purchased from MUCSAT (Egypt). Kjeldahl catalyst (6.25% $CuSO_4.5H_2O$) was purchased from Panreac Quimice S.A. Co. (Australia).

2.2. Methods

2.2.1. Preparation of P(AN-co-MMA) nanoparticles

The poly (acrylonitrile-co-methyl methacrylate) was prepared by simple precipitation polymerization of acrylonitrile (AN) and methyl methacrylate (MMA) = 1:1 using (0.01 M) potassium per-sulfate ($K_2S_2O_8$) as initiator. Unless otherwise stated, to the reactor fitted with a magnetic stirrer, the mixed monomers and the co-solvent from distilled water and ethanol as a solvent were added, and followed by stepwise injection of initiator. Temperature was kept at 55 °C for 4 h. The polymer was isolated by centrifugation at high speed (14,000 rpm) and washed successively with ethanol-distilled water mixture at 55 °C. The product was then dried in an oven at 55 °C for 24 h. The white powder was obtained as a product (Scheme 1)

The obtained polymerization yield was calculated from the following equation:

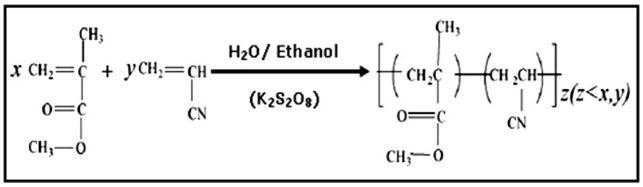

Scheme 1 Synthesis copolymer of P(AN-co-MMA) nanoparticles.

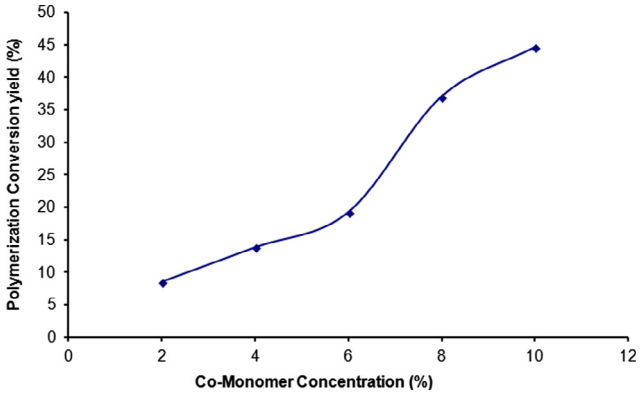

Figure 1 Effect of comonomer concentration of (*AN&MMA*) on the polymerization conversion yield [Reaction condition:Comonomer concentration (1:1) from (*AN:MMA*), 0.01 M $K_2S_2O_8$, cosolvent solution (1:1) from (*H_2O:Ethanol*), 55 °C, 4 h].

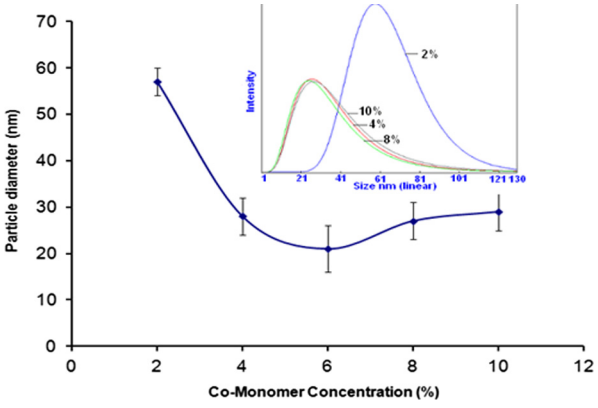

Figure 2 Influence of the comonomer content on the effective diameter of (*P(AN-co-MMA)*) [Reaction condition:Comonomer concentration (1:1) from (*AN:MMA*), 0.01 M $K_2S_2O_8$, cosolvent solution (1:1) from (*H_2O:Ethanol*), 55 °C, 4 h].

$$Y\ (\%) = \frac{W}{Z} \times 100$$

where W = Weight of copolymer, Z = wt of MMA + wt of AN.

2.2.2. Characterization of copolymer of P(AN-co-MMA) nanoparticles

To verify the chemical structure and study the composition of P(AN-co-MMA) nanoparticles prepared under different poly-

merization conditions, the following techniques and methods were used.

2.2.3. FT-IR spectroscopic analysis

The structure of P(AN-co-MMA) was analyzed by FT-IR spectra. In an atypical procedure, ''Samples were mixed with KBr to make pellets. FT-IR spectra in the absorbance mode were recorded using FT-IR spectrometer (Shimadzu FTIR-8400 S, Japan), connected to a PC, and data were analyzed by IR Solution software, Version 1.21'' (Mohy Eldin et al., 2012).

2.2.4. Thermal characterization (TGA)

''The thermal degradation behaviors of P(AN-co-MMA) were studied using Thermo Gravimetric Analyzer (Shimadzu TGA–50, Japan); instrument in the temperature range from 20 °C to 600 °C under nitrogen at a flow rate of 20 ml/min and at a heating rate of 10 °C/min'' (Mohy Eldin et al., 2012).

2.2.5. Morphological characterization (SEM)

The surface morphology of P(AN-co-MMA) was observed after coating with gold with the help of a scanning electron microscopy (Joel Jsm 6360LA, Japan) at an accelerated voltage of 20 kV.

2.2.6. Particle size analysis

Particle size of P(AN-co-MMA) was analyzed by using Submicron Particle Size Analyzer (Beckman Coulter – USA). The sample dispersed in water, at a temperature 20 °C, of viscosity 1.002 and refractive index 1.33.

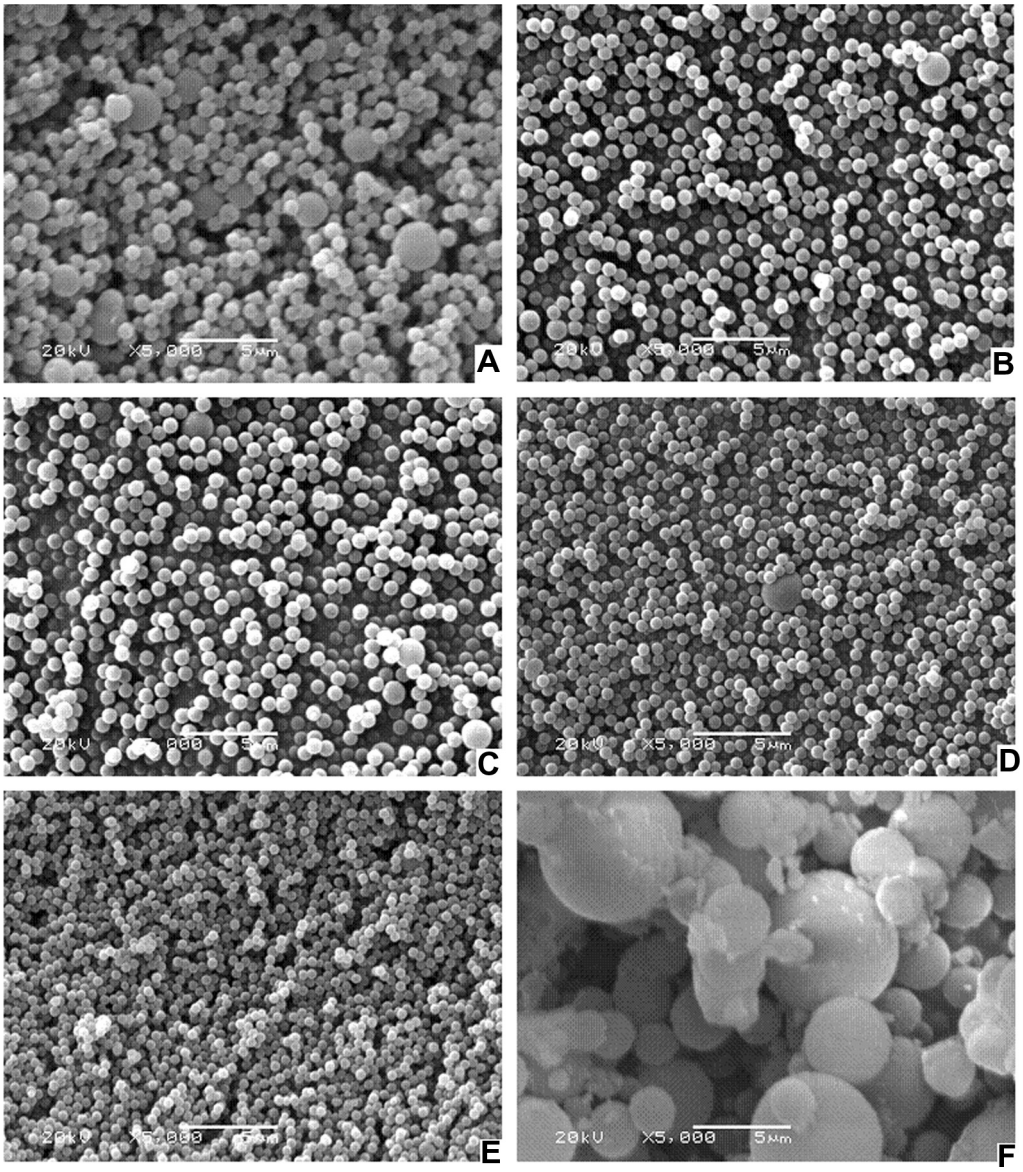

Figure 3 SEM photographs of *P(AN-co-MMA)* nanospheres prepared with comonomer concentration; (A) 2%, (B) 4%, (C) 6%, (D) 8%, (E) 10%, and (F) 20% [Reaction condition:Comonomer concentration (1:1) from (*AN:MMA*), 0.01 M $K_2S_2O_8$, cosolvent solution (1:1) from (*H_2O:Ethanol*), 55 °C, 4 h].

2.2.7. Determination of nitrogen on copolymer of P(AN-CO-MMA) nanoparticles by Kjeldahl method

In an atypical procedure, this method consists in mineralizing the sample with concentrated sulfuric acid and alkalinizing with NaOH. The ammonium liberated is carried by distillation and recovered in boric acid. The subsequent titration with HCl allows the calculation of the amount of ammonium in the sample.

To a sample of 0.5 g, was added a sample of 1 g of copper sulfate catalyst, 10 ml of sulfuric acid at 96% (d = 1.84), and some granules of glass. Put the digestion tube with the sample into the Bloc-digest with the fume removal working. Do the digestion at a temperature between 350 °C and 420 °C. To 50 ml of boric acid was added mixed of indicator in an Erlenmeyer flask. The distillation has to be extended for enough time in order to be distilled for a minimum of 150 ml, approximately between 5 min and 10 min. Titrate the distilled obtained with HCl 0.25 N until the solution changed from green to violet color (Mohy Eldin et al., 2012).

Calculate the quantity of nitrogen detected by means of formulae:

$$\text{Nitrogen } (\%) = \frac{1.4 \times (V_1 - V_0) \times N}{P}$$

where P = weight g of sample, V_1 = HCl consummation on titration (ml), V_0 = HCl consummation on blank (ml) and N = normality of HCl.

Conversion of nitrogen percentage to weight is done using the following formula.

$$100 \rightarrow N\%$$
$$W \rightarrow X$$
$$X = \frac{W \times N}{100}$$

where X = weight g of nitrogen in sample, W = weight of sample, and N = percentage of nitrogen.

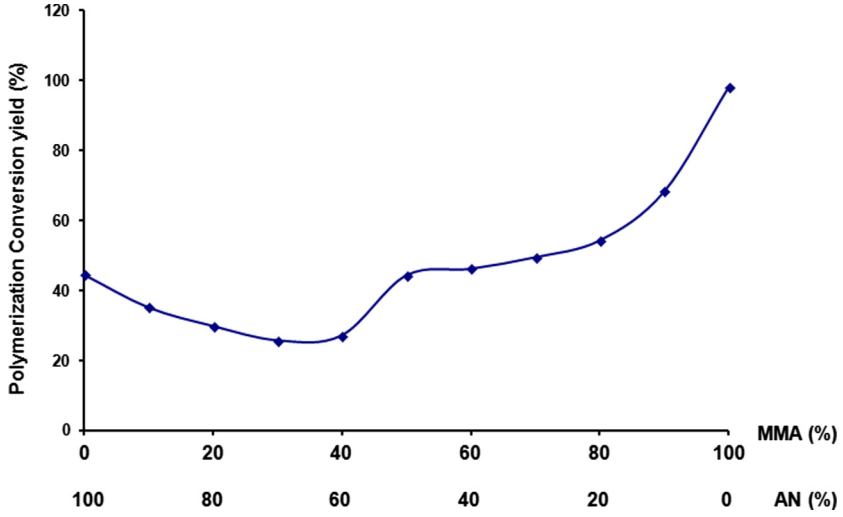

Figure 4 Effect of comonomer composition (*AN:MMA*) on the polymerization conversion yield [Reaction condition:10% Comonomer concentration from (*AN:MMA*), 0.01 M $K_2S_2O_8$, cosolvent solution (1:1) from (H_2O:*Ethanol*), 55 °C, 4 h].

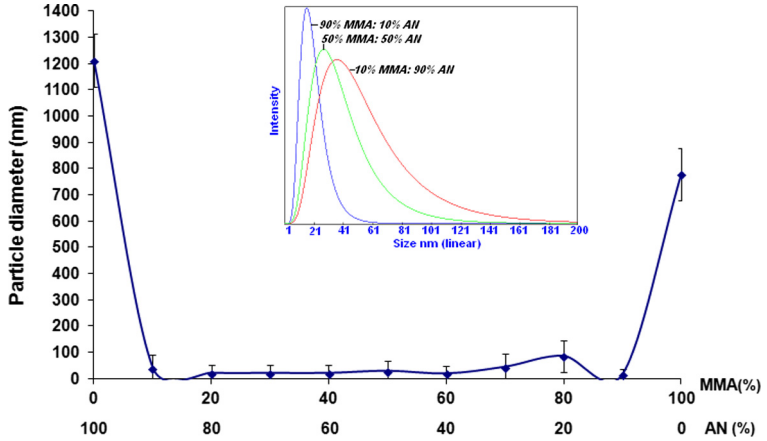

Figure 5 Influence of the comonomer composition on the effective diameter of (*P(AN-co-MMA)*), [Reaction condition:10% Comonomer concentration from (*AN:MMA*), 0.01 M $K_2S_2O_8$, cosolvent solution (1:1) from (H_2O:*Ethanol*), 55 °C, 4 h].

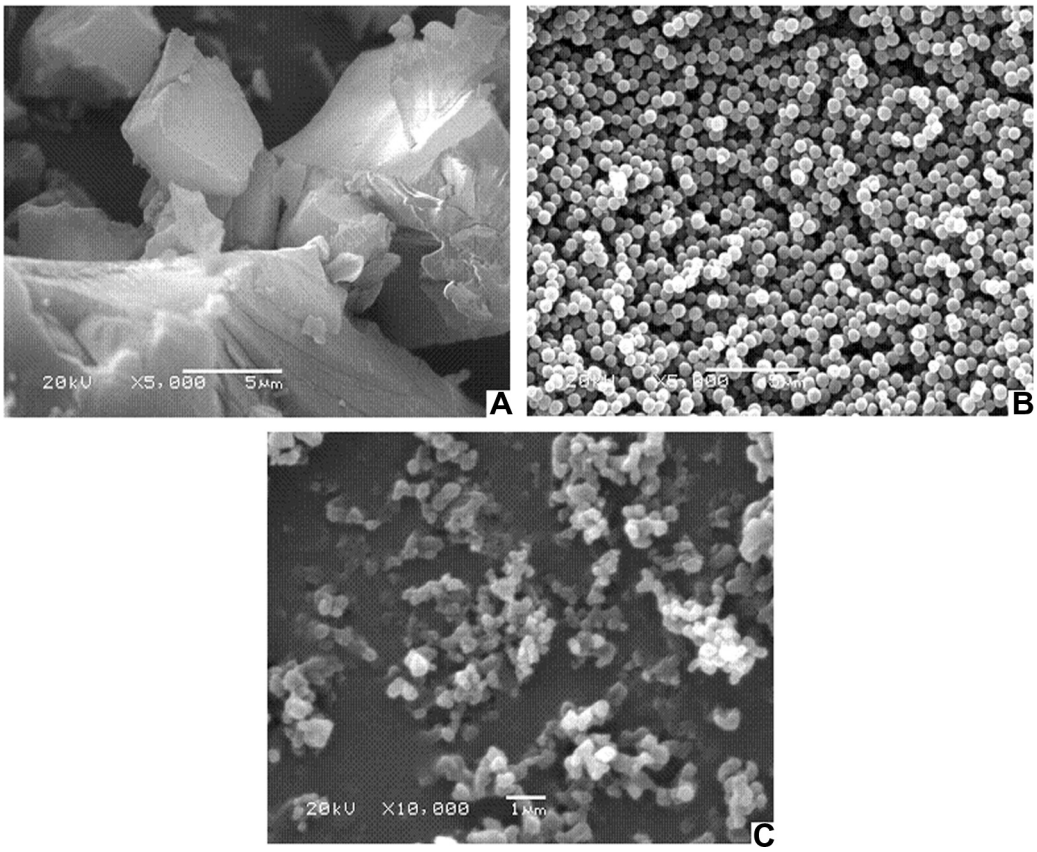

Figure 6 SEM photographs of (A) *PAN*, (B) *P(AN-co-MMA)* nanospheres, (C) *PMMA* [Reaction condition:10% monomer concentration from (*AN, MMA and AN:MMA*), 0.01 M $K_2S_2O_8$, cosolvent solution (1:1) from (H_2O:*Ethanol*), 55 °C, 4 h].

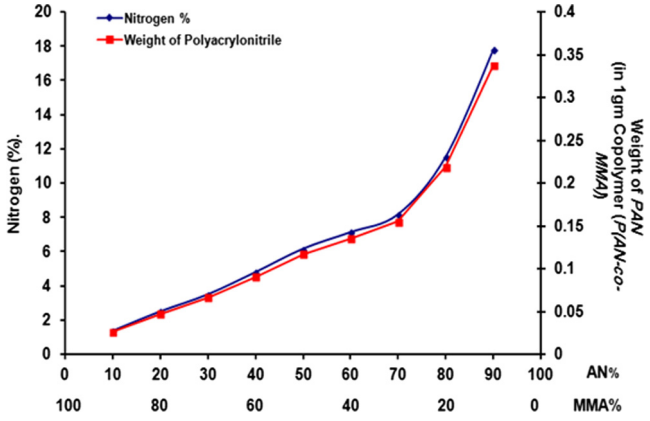

Figure 7 Effect of acrylonitrile concentration on the composition of *P(AN-co-MMA)* nanospheres and determination of nitrogen and weight of *PAN* (in 1gm copolymer (*P(AN-co-MMA)*) by Kjeldahl methods.

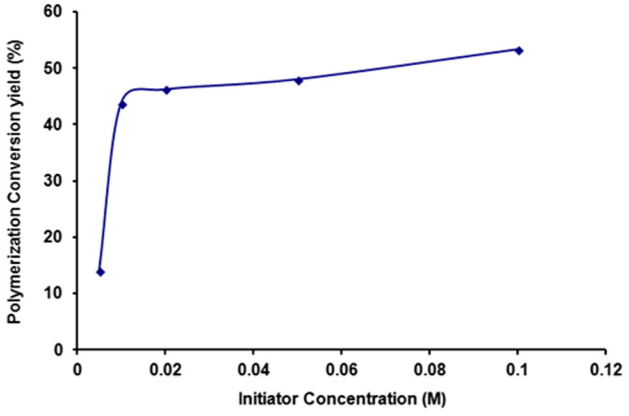

Figure 8 Effect of initiator concentration ($K_2S_2O_8$) on the polymerization conversion yield [Reaction condition:10% Comonomer concentration (1:1) from (*AN:MMA*), $K_2S_2O_8$, co-solvent solution (1:1) from (H_2O:*Ethanol*), 55 °C, 4 h].

Then to calculate the weight of acrylonitrile

$$\text{M.wt(AN)} \rightarrow \text{M.wt(N)}$$

$$\text{W of(AN)} \rightarrow X$$

$$\text{W(AN)} = \frac{\text{M.Wt(AN)} \times X}{14}$$

where W of (AN) = weight of acrylonitrile, M.wt (AN) = molecular weight g of acrylonitrile, X = weight g of nitrogen in sample.

3. Results and discussion

The impact of different polymerization conditions such as comonomer concentration and composition, polymerization time, polymerization temperatures, initiator concentration and co-solvent composition on the polymerization yield and particle size and its morphology structure was studied. Also, the effect of the feed comonomer system composition on the

composition of the prepared copolymers was monitored. Finally, the formation of copolymer was verified by FT-IR and TGA analysis.

3.1. Copolymerization process

3.1.1. Effect of the comonomer concentration

Fig. 1 shows the effect of variation in comonomer concentration on the polymerization conversion yield obtained by estimating the amount of monomers converted to copolymer. It is clear that the conversion yield% of the comonomers reaches its highest value by using 10% comonomer concentration. The curve has two stages. The first stage is linear increment of yield in the comonomer concentration from 2% to 6%. The second stage, in the comonomer concentration range from 6% to 10%, the rate of increment turned to be exponential. This behavior may be due to the concentration of reactants in the polymerization medium becoming higher which increases the probability of the molecular collision of reactants leading to an increase in the conversion yield%.

Fig. 2 depicts the effect of monomer concentration on the formed particle size. Particle sizes are getting smaller with the gradual increase of monomer concentration.

Qiana et al. (2006) have reported that, increase in both the surface charges and surface hydrophilicity may be the main reasons behind reducing the particle size with increase in monomer concentration. On the other hand, variation of type of charges over monomer surfaces and produced copolymer may have a direct impact on the prepared particle size.

Fig. 3 represents results of the scanning electron microscopy (SEM) photographs. As seen, spherical particles are obtained. The images show the successful synthesis of copolymer nanoparticles. As the copolymer concentration increased up to 10%, the size of P(AN-co-MMA) nanosphere decreased. This could be explained as previously reported; "nanospheres decreased due to the favorable formation of more primary nuclei in the early stage of polymerization" Lee et al. (2009).

Fig. 3(F) is a representative photograph of the P(AN-co-MMA) particles prepared with 20% comonomer for a comparison. By observing the spherical particles, the final particle size distributions of the P(AN-co-MMA) particles are broad, and the spherical form starts to destroy.

3.1.2. Effect of the comonomer (AN:MMA) composition

In exploring the effect of ratio between MMA monomer and AN monomer in the comonomer solution, on the conversion yield, comonomer solutions with different compositions have been polymerized (Fig. 4). For better understanding, both AN and MMA have been polymerized individually under the same conditions and their conversion yields were obtained. From the obtained data it is obvious that MMA is more reactive than AN where 100% of MMA was converted to polymer compared with 45% only of AN. Two trends have been noticed as seen in Fig. 4. The first trend is linear decrement of the conversion yield of comonomer with MMA from 0% to 40% amount with increase in the amount of AN monomer in the range 60–100%. The second part or trend of the curve started from MMA from 50% to 100% in which the conversion yield of comonomer increment rate was found higher. This behavior is explained according to the optimum ratio between AN monomer and MMA monomer. This result can be attributed to chain transfer reactions to ligand (Shen et al., 1996). It must be borne in mind that the solubility of both individual monomers in the cosolvent solution components is different. Where AN solubility in water is reaching to 7%, the solubility of MMA is only 3%. However, both monomers are soluble in ethanol. The persulfate solubility in ethanol is very limited while it is completely soluble in water. The combination of all these factors leads finally to the obtained results.

Fig. 5 illustrates the effect of AN and MMA initial concentration in the feeding comonomer solution on the size and size distribution of the P(AN-co-MMA) nanoparticles. Data show an increase in particle size from approximately 40 to 1212 nm with increase in the concentration of AN from 10% to 100%. On the other hand, increasing the concentration of MMA from 10% to 90% will lead to spherical and narrow size particles (Boguslavsky et al., 2005).

Fig. 6 shows SEM images of PAN, PMMA, and P(AN-co-MMA), from the figure, the changes in the surface morphology of copolymer nanoparticles and formation spherical particles are clear. The images show the successful synthesis of copolymer nanoparticles when mixing the MMA with AN.

The Kjeldahl method can measure nitrogen in P(AN-co-MMA) nanospheres. It is used for determining the content of polyacrylonitrile in different P(AN-co-MMA) nanospheres prepared with differed comonomer compositions in this study. Fig. 7 illustrates the effect of AN concentration on the nitrogen contents of the P(AN-co-MMA) nanosphere copolymers. This figure shows that when the concentration of AN is changed from 10% to 90% (v/v), the nitrogen content increases from approximately 2% to 18%. On the other hand, the polyacrylonitrile varied from 5 to 34%, weight percent, of copolymer composition. These results reflect the effect of reactivity ratio difference between the two monomers in the copolymers.

3.1.3. Effect of the initiator concentration

Fig. 8 shows the effect of variation of $K_2S_2O_8$ concentration on the polymerization conversion yield. Linear increase in

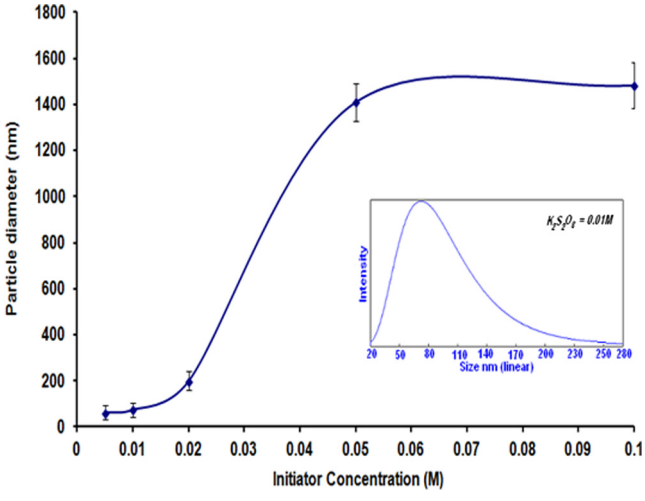

Figure 9 Influence of the initiator concentration ($K_2S_2O_8$) on the effective diameter of (*P(AN-co-MMA)*) [Reaction condition:10% Comonomer concentration (1:1) from (*AN:MMA*), $K_2S_2O_8$, cosolvent solution (1:1) from (H_2O:*Ethanol*), 55 °C, 4 h].

the conversion yield has been observed with increasing the $K_2S_2O_8$ concentration up to 0.01 M. Slight increase in the conversion yield was noticed over increase in the concentration up to 0.1 M. The results signify that increasing the $K_2S_2O_8$ concentration up to 0.1 M is accompanied by enhancement in the conversion yield of P(AN-co-MMA) copolymer. It should be noted however, that the magnitude of this enhancement is striking up to 0.01 M $K_2S_2O_8$ and not so at higher $K_2S_2O_8$ concentrations i.e., 0.05 M and 0.1 M. Increment of conversion yield of the copolymer by increasing $K_2S_2O_8$ concentration up to 0.01 M could be interpreted in terms of the contribution of the primary free radical species participation mainly in the initiation of the polymerization when $K_2S_2O_8$ range from 0.005 to 0.01 M was used, which exhibits higher enhancement in the % total conversion within the range studied.

Fig. 9 shows the effect of initiator concentration on the P(AN-co-MMA) nanoparticle size and size distribution in the presence of 10% (v/v) (AN-co-MMA).

Data show that, large particles with a wide size distribution have formed with increase in the initiator concentration. For example, in the presence of 0.005 and 0.1 M ($K_2S_2O_8$), the particle sizes are 63 and 1485 nm respectively. The results come in agreement with the previous studies reported by Shen et al. (1996) and Paine et al. (1990). According to their explanation, oligomeric radical concentration and consequently number of P(AN-co-MMA) chains will be increased as a result of increasing initiator concentration. Boguslavsky et al. (2005) have

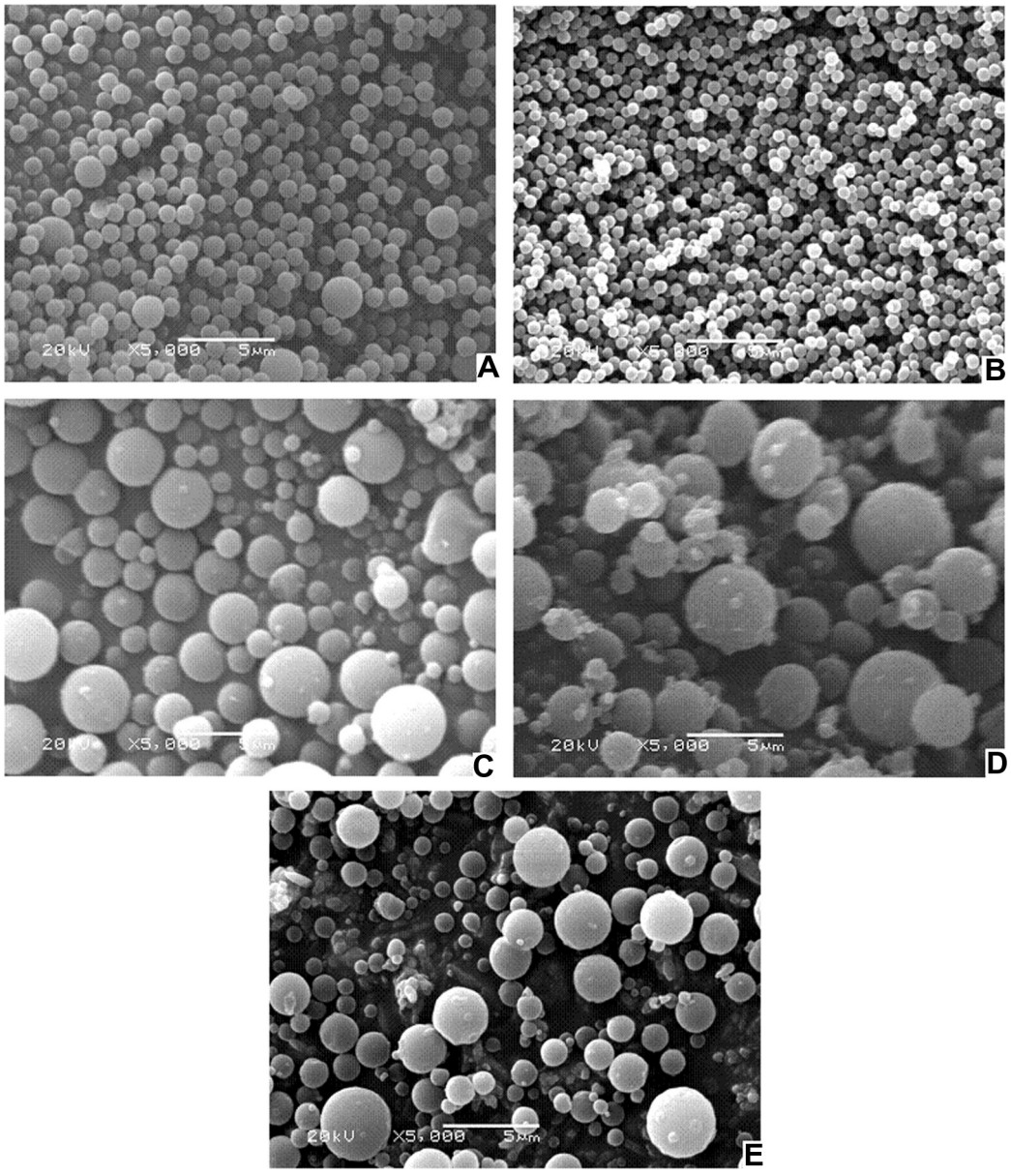

Figure 10 SEM photographs of *P(AN-co-MMA)* nanospheres prepared with initiator concentration; (A)*0.005 M*, (B) *0.01 M*, (C) *0.02 M*, (D) *0.05 M*, and (E) *0.1 M* [Reaction condition:10% Comonomer concentration (1:1) from (*AN:MMA*), cosolvent solution (1:1) from (*H_2O:Ethanol*), 55 °C, 4 h].

reported that, ''this may lead to an increase in the number of P(AN-co-MMA) nanoparticles (more nuclei) and an increase in their size (more P(AN-co-MMA) chains participating in the growing process). Moreover, a higher initiator concentration increases the growth rate of the oligomeric chains, thus favoring secondary nucleation during the particle growth stage, and this may account for the broad particle size distribution above 0.02 M ($K_2S_2O_8$)''.

Fig. 10 shows SEM images of P(AN-co-MMA) copolymer nanoparticles prepared using various initiator concentrations. As shown in the figure, using lower ($K_2S_2O_8$) concentrations has a better impact to have narrow particle size distribution. This impact has been reduced at higher ($K_2S_2O_8$) concentrations. Accordingly, the best particle size distribution was obtained with 0.01 M ($K_2S_2O_8$). Tuncel (2000) studied the Emulsion copolymerization of styrene and poly(ethylene glycol) ethyl ether methacrylate. He found the same trend where the average particle size increased with increasing ($K_2S_2O_8$) concentration. Similar trend has been observed by Tanrisever et al. (1996) during their study of Kinetics of emulsifier-free emulsion polymerization of methyl methacrylate. They attributed the obtained results to increase in the ionic strength of the aqueous phase which strongly affected the particle size.

3.1.4. Effect of the cosolvent composition

The effect of variation of cosolvent composition on the polymerization conversion yield has been performed by studying the effect of variation of H_2O amount (Fig. 11).

Zhang et al. (2004) have reported the use of ethanol/water media in the copolymerization of methyl methacrylate and acrylic acid. They have declared that, ''the solubility parameter was chosen to estimate the miscibility of each ingredient involved in the polymerization system. If the polar part of each ingredient was not taken into account, the monomers were less miscible with the media and tended to form monomer microdroplets under proper agitation, and continuously and stably deposition in the media. The deposition is micromorphicly like oil-in-water''.

However, this is not the case at present since the cosolvent is able to dissolve completely the comonomer.

The determined factor here is the capability of the cosolvent composition to swell, stabilize or even dissolve the formed copolymers. The presence of ethanol, which is known as a solvent for PMMA, acts somehow as a stabilizer for the copolymers. The stability effect depends on the percent of PMMA in the formed copolymer particles. Increase in the PMMA ratio in the formed copolymer will lead to some kind of higher stability of the particles and in sequence derived to the formation of bigger particle size.

Fig. 12 shows the number-average particle diameter of nanospheres prepared using water and ethanol as the media at 55 °C. It has been reported that, solubility in cosolvent has an important effect on the size of produced nanosphere (Lok and Ober, 1985). In pure alcohol, the largest particle size was obtained (777 nm). On the other hand, it was observed that, decreasing alcohol concentration has led to a smaller particle size as shown in Fig. 12. This property was related to the polarity of the solvent system, and when using the cosolvent in the range from 20/80 ethanol/water to 60/40 ethanol/water, the size of nanospheres in the range from 30 to 50 nm; respectively.

Experimental conditions and SEM images of resulting particles are presented in Fig. 13; we already demonstrated the effect of solvent polarity on the final particle size. The ionic strength of the reaction medium affects the morphology and the size of particles. Therefore, the amount of ethanol added should be less than that of the amount of water, in order for both systems to have identical solvent polarity. The effect of ethanol on the morphology and the size of grown particles is shown in Fig. 13. The excess amount of ethanol however, caused aggregated particles Fig. 13 (E,F).

3.1.5. Effect of the polymerization temperature

The effect of variation in polymerization temperature was studied by changing the reaction temperature from 35 °C to 70 °C and keeping other reaction conditions constant, as shown in Fig. 14. Increase in temperature led to increase in the polymerization rate. This could be explained by the fact that, increasing the temperature will lead in enhancing the decomposition of initiator, increasing the collision chance between (MMA & AN) comonomer and $K_2S_2O_8$ and also the propagation rate as reported by Zhang et al. (2004). On

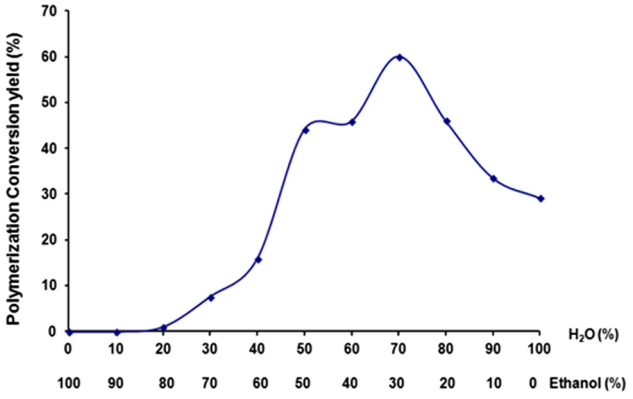

Figure 11 Effect of cosolvent ratio (*H_2O:Ethanol*) on the polymerization conversion yield, [reaction condition:10% Comonomer concentration (1:1) from (*AN:MMA*), 0.01 M *$K_2S_2O_8$*, cosolvent solution (*H_2O:Ethanol*), 55 °C, 4 h].

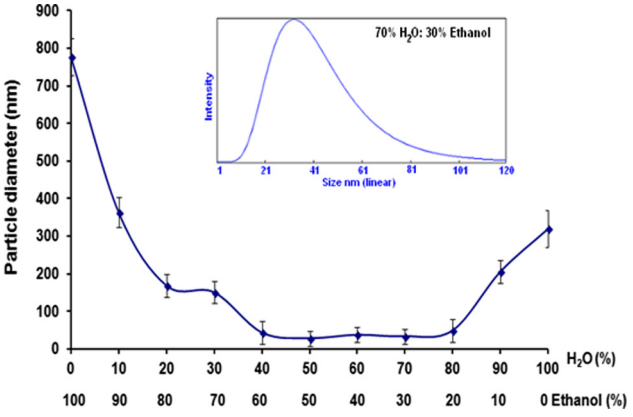

Figure 12 Influence of the cosolvent ratio (*H_2O&Ethanol*) on the effective diameter of (*P(AN-co-MMA)*) [Reaction condition:10% Comonomer concentration (1:1) from (*AN:MMA*), 0.01 M *$K_2S_2O_8$*, cosolvent solution (*H_2O:Ethanol*), 55 °C, 4 h].

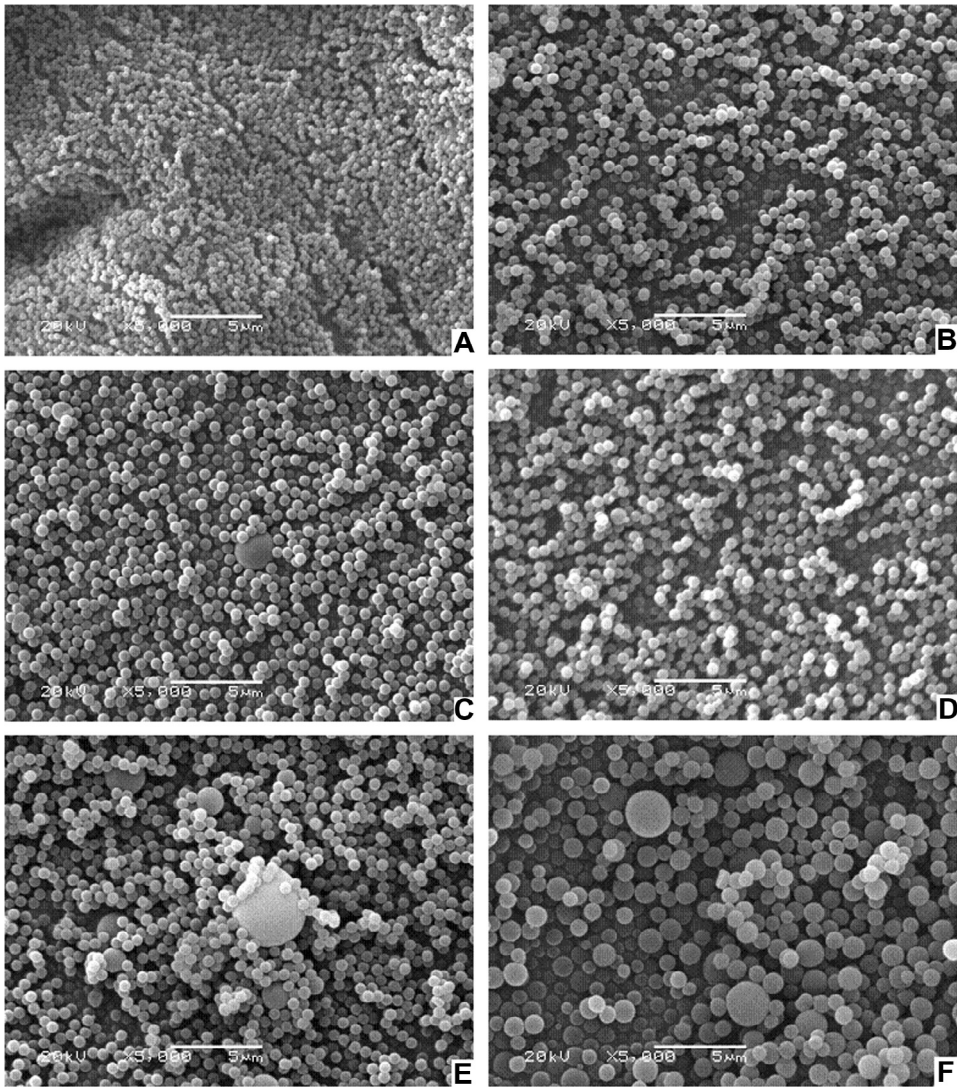

Figure 13 SEM photographs of *P(AN-co-MMA)* nanospheres prepared with cosolvent concentration; (A) 100% H_2O, (B) 90% H_2O:10% *ET.OH*, (C) 80% H_2O:20% *ET.OH*, (D) 50% H_2O:50% *ET.OH*, (E) 40% H_2O:60% *ET.OH*, and (F) 30% H_2O:70% *ET.OH*, [Reaction condition:10% comonomer concentration (1:1) from (*AN:MMA*), 0.01 M $K_2S_2O_{8,}$ 55 °C, 4 h].

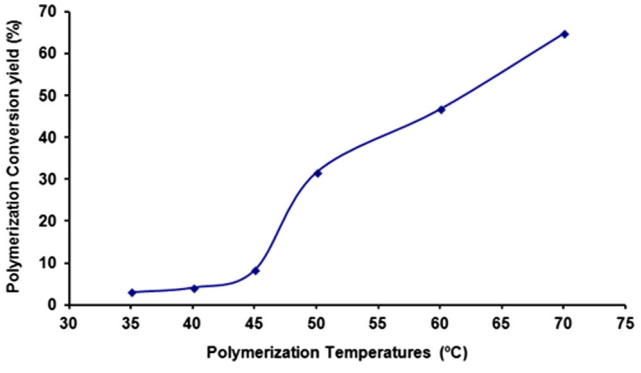

Figure 14 Effect of polymerization temperatures on the polymerization conversion yield [Reaction Condition:10% comonomer concentration (1:1) from (*AN:MMA*), 0.01 M $K_2S_2O_{8,}$ cosolvent solution (1:1) (H_2O:*Ethanol*), 4 h].

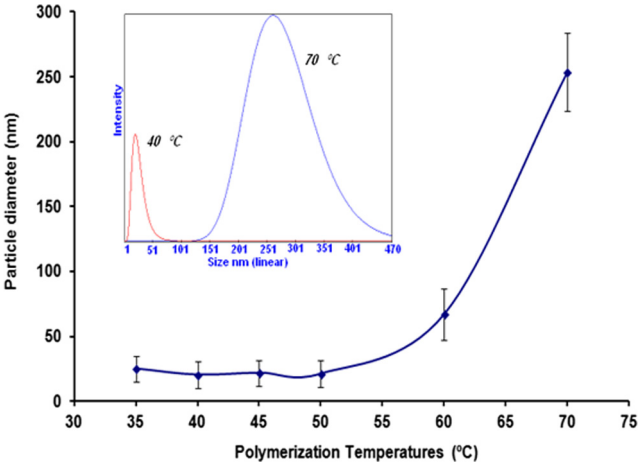

Figure 15 Influence of the polymerization temperatures on the effective diameter of (*P(AN-co-MMA)*), [Reaction condition:10% Comonomer concentration (1:1) from (*AN:MMA*), 0.01 M $K_2S_2O_{8,}$ cosolvent solution (1:1) (H_2O:*Ethanol*), 4 h].

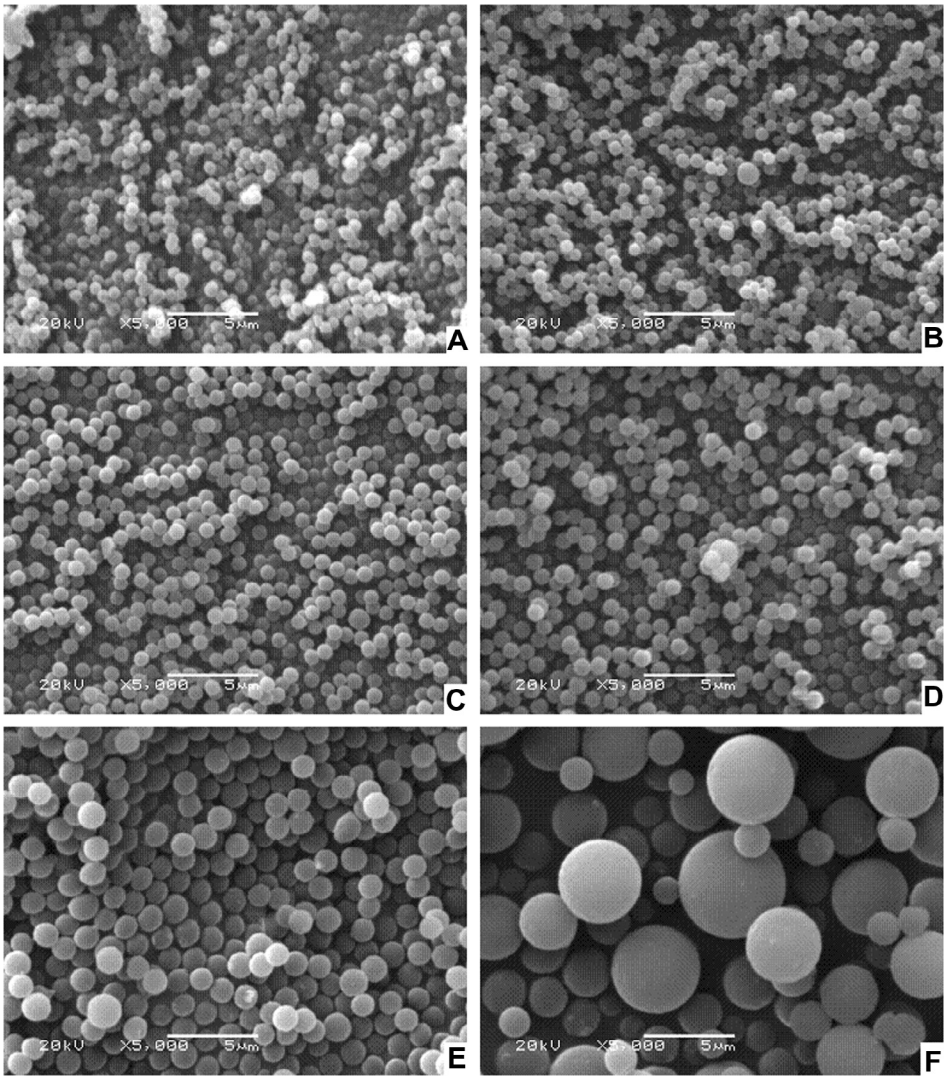

Figure 16 SEM photographs of *P(AN-co-MMA)* nanospheres prepared with polymerization temperatures; (A)*35 °C*, (B) *40 °C*, (C) *45 °C*, (D) *50 °C*, (E) *60 °C*, and (F) *70 °C*, [Reaction condition:10% Comonomer concentration (1:1) from (*AN:MMA*), 0.01 M $K_2S_2O_8$, cosolvent solution (1:1) (*H_2O:Ethanol*), 4 h].

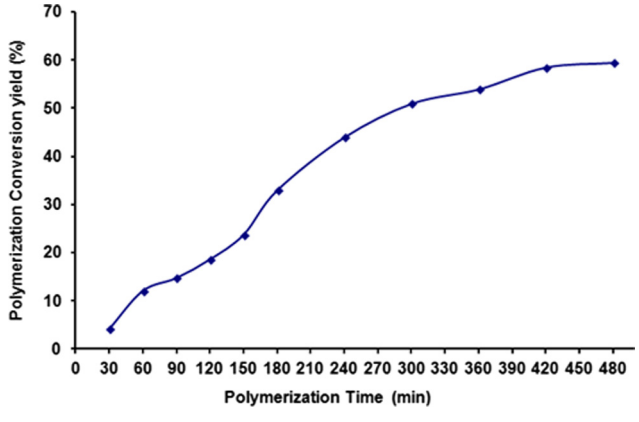

Figure 17 Effect of polymerization time on the polymerization conversion yield [Reaction condition:10% comonomer concentration (1:1) from (*AN:MMA*), 0.01 M $K_2S_2O_8$, cosolvent solution (1:1) (*H_2O:Ethanol*), 55 °C].

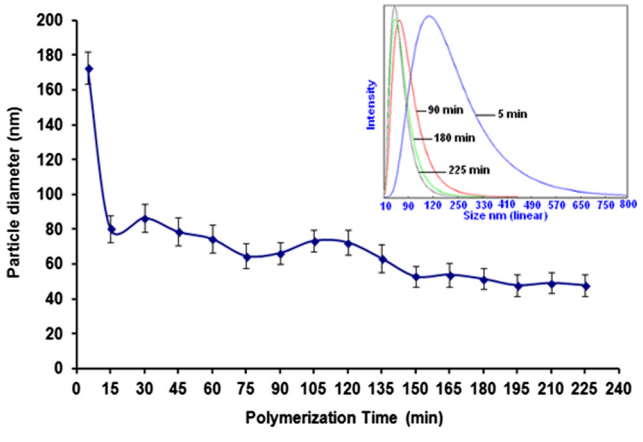

Figure 18 Influence of the polymerization times on the effective diameter of (*P(AN-co-MMA)*) [Reaction condition:10% Comonomer concentration (1:1) from (*AN:MMA*), 0.01 M $K_2S_2O_8$, cosolvent solution (1:1) (*H_2O:Ethanol*), 55 °C].

the other hand, the low conversion yield recorded at low temperatures is mainly due to the low amount of generated radical and consequently, the slow redox reaction between $K_2S_2O_8$ and (MMA & AN) comonomer.

Fig. 15 illustrates the effect of variation of polymerization temperature on the P(AN-co-MMA) nanoparticle size. This figure shows the variation of particle sizes at different polymerization temperature from 35 °C to 70 °C. Starting from 35 °C, there is a constant growth in the particle size, until the temperature reaches to 50 °C. At 60–70 °C, there is a sharp increase in the size of the particles from 67 nm to 235 nm in the polymerization process. Same behavior has been previously reported in the case of dispersion polymerization of styrene (Margel and Bamnolker, 1996; Baines et al., 1996), methyl methacrylate (Shen et al., 1994), hydroxyethyl methacrylate (Horak et al., 1999), and of styrene with butyl acrylate (Sáenz and Asua, 1998).

Boguslavsky et al. (2005) have explained the effect of changing temperature on the produced particle size. They declared that, increase in the temperature will have the same effect as increase in the initiator concentration. This will eventually lead to increase in the polymerization rate and the particle size. In addition to that, Boguslavsky et al. (2005) have stated that ''contrary to increasing the initiator concentration, increasing the temperature leads to an increase in the oligoradical reactivity and a decrease in their half-life period, thus achieving a faster particle growth rate and a more rapid attainment of their maximal size''. Shen et al. (1994) have found the same results during their studies of mechanism of particle formation during dispersion polymerization of methyl methacrylate. It has been reported that, the high concentration of precipitated oligomer chains and high solvency of the continuous phase are the main reasons behind increasing the critical chain length. (Boguslavsky et al., 2005)

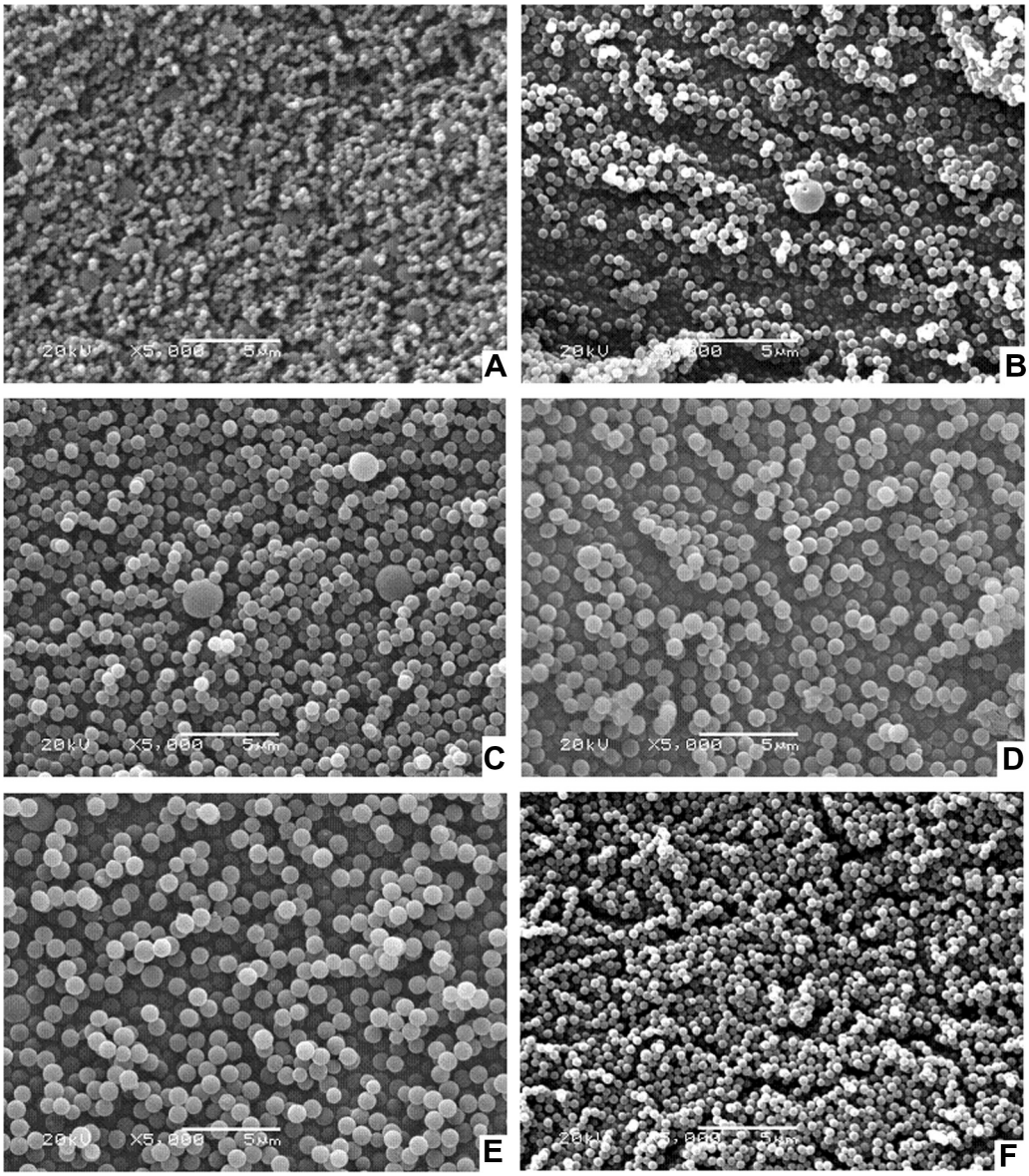

Figure 19 SEM photographs of *P(AN-co-MMA)* nanospheres prepared with polymerization times [Reaction condition:10% Comonomer concentration (1:1) from (*AN:MMA*), 0.01 M $K_2S_2O_8$, cosolvent solution (1:1) (H_2O:*Ethanol*), 55 °C].

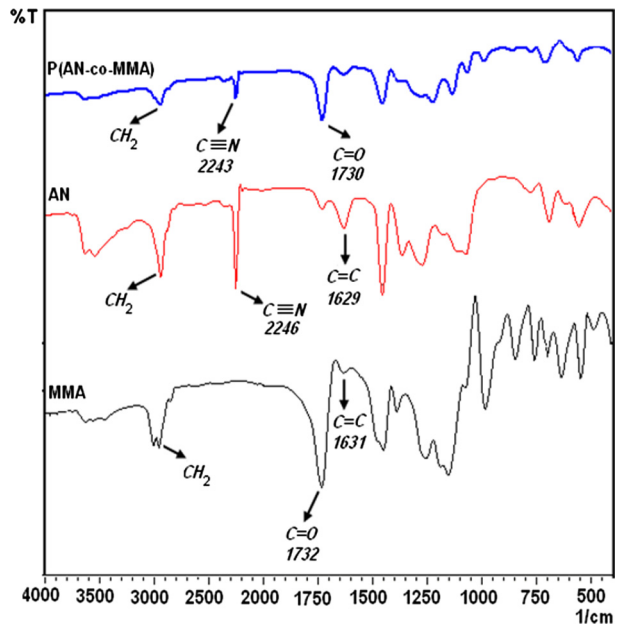

Figure 20 FTIR spectra for *AN*, *MMA* and *P(AN-co-MMA)* with comonomer compassion of (*AN:MMA*) (1:1) in the range of 450–4000 cm^{-1}.

Fig. 16 shows SEM images of P(AN-co-MMA) copolymer nanoparticles, prepared under different polymerization temperatures. The figure shows that the average particle diameter increased with increasing the polymerization temperature. At high polymerization temperature, due to low concentration of high molecular weight chains in the medium, a few nuclei were produced, leading to a few larger sizes (Ki-Chang Lee et al., 2004).

3.1.6. Effect of the polymerization time

The effect of variation in polymerization time on the polymerization conversion yield has been studied (Fig. 17). A linear increase in the conversion yield has been observed with a reaction time increase up to 300 min. Further upon increase of reaction time to 480 min, the conversion yield increased linearly but with lower rates. With the increase in reaction time, the concentration of (MMA & AN) comonomer and free radicals in the system increased and resulted in the increase of P(MMA & AN) nanoparticles. With polymerization reaction progress, both initiator and comonomers are consumed. In addition, the absence of agitation reduces the chances of collision between formed free redials and left free monomer unites, both factors affect, negatively the polymerization conversion yield which depends mainly on the last stage of reaction on the diffusion of free radicals and monomer units.

Fig. 18 shows the variation of particle size with reaction time at the temperature 50 °C. Data show three stages till reaching their final stable size; beginning with a sharp decrease in the particle size within the first 15 min of the polymerization, followed by a moderate decrease in their size till they reach their final stable size of 70–50 nm after approximately 60 min of reaction. This indicates the termination of polymerization process (Boguslavsky et al., 2005).

Fig. 19 represents results of the scanning electron microscopy (SEM) photographs of the P(AN-co-MMA) nanospheres prepared with various polymerization times of 30, 60, 90, 120, 150, and 240 min. As usual, spherical particles are obtained. The images show the successful synthesis of copolymer nanoparticles, as the polymerization time increased, the size of P(AN-co-MMA) nanospheres decreased due to the favorable formation of more primary nuclei in the early stage of polymerization (Lee et al., 2009).

Fig. 19(F) is a representative photograph of the P(AN-co-MMA) particles prepared at 240 min. By observing the spherical particles, the final particle size distributions of the P(AN-co-MMA) particles are nanospherical and Homogeneous in size.

3.2. Nanoparticles characterization

3.2.1. FT-IR analysis

Fig. 20 presents the FTIR spectra of polymers, (PAN) and (PMMA), and their copolymer, P(AN-co-MMA). Typical characteristic peaks at 1629 $cm^{-1}$and 2246 cm^{-1}, which correspond to the bonds C═C and C≡N respectively have been recorded for PAN polymer (Rao et al., 2008; Zhou et al., 2008). The characteristic peaks at 1631 cm^{-1} and 1732 cm^{-1}, which correspond to the bonds C═C and C═O respectively have been recorded for PMMA polymer (Rajendran et al., 2003; Zhang et al., 2007b). For P(AN-co-MMA), the presence of peaks at 1730 cm^{-1} for and 2243 cm^{-1} for and disappearance of peaks at 1629 or 1631 cm^{-1} can be easily seen. As previously reported, this indicated that copolymerization process has been achieved through the breaking of double bonds in both monomers (AN) and (MMA) (Zhou et al., 2008).

3.2.2. TGA analysis

The thermal stability of the P(AN-co-MMA) nanoparticles was analyzed by thermogravimetry under N_2 atmosphere, from room temperature to 600 °C at a heating rate of 10 °C min^{-1}. The result in Fig. 21 shows no mass loss and thermal stability below 306 °C for P(AN-co-MMA) compared to PMMA and PAN, which showed a thermal stability up to 265 °C and 269 °C, respectively (Zhang and Zhang, 2007). Apparently, the formation of copolymer has enhanced the thermal stability of both individual polymers (Zhou et al., 2008).

3.2.3. X-ray diffraction analysis

Fig. 22 shows the XRD patterns of PMMA, PAN and P(AN-co-MMA) nanoparticles. In Fig. 22(a), one relatively strong diffraction peak is found at $2\theta = 14.5°$ for PMMA, which reflects the crystallization of polymer (Zhang et al., 2007a). The X-ray diffraction pattern of the PAN involves two narrow peaks at $2\theta = 16.7°$ and 25.5° Fig. 22(b). P(AN-co-MMA) nanoparticles also have diffraction peaks, indicating that P(AN-co-MMA) is characteristic of crystallization, as shown in Fig. 22(c). This result is consistent with that reported by Liao et al. (2009) and Shi et al. (2005). As shown in Fig. 22(c) it can be found by comparing Fig. 22(b) and (c) that the diffraction peaks of P(AN-co-MMA) are weaker and broader than those of PAN, indicating that P(AN-co-MMA) has lower crystallinity than PAN, PMMA is amorphous, thus "the addition of the monomer (MMA) to (AN) may reduce the crystallinity and increase the amorphous nature of the copolymer" (Liao et al., 2009).

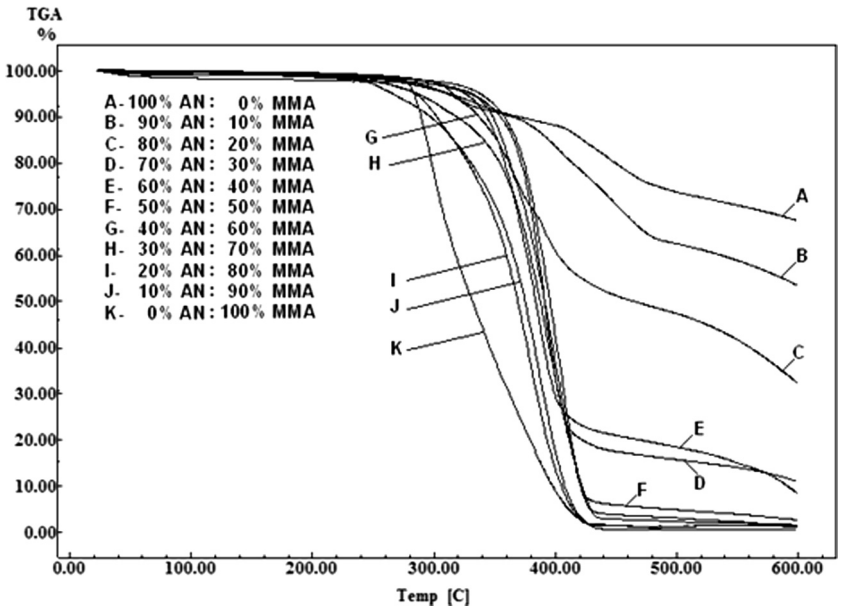

Figure 21 TGA curve for *PAN*, *PMMA* and *P(AN-co-MMA)* with different monomer compassion, from room temperature to 600 °C at a heating rate of 10 °C min^{-1}.

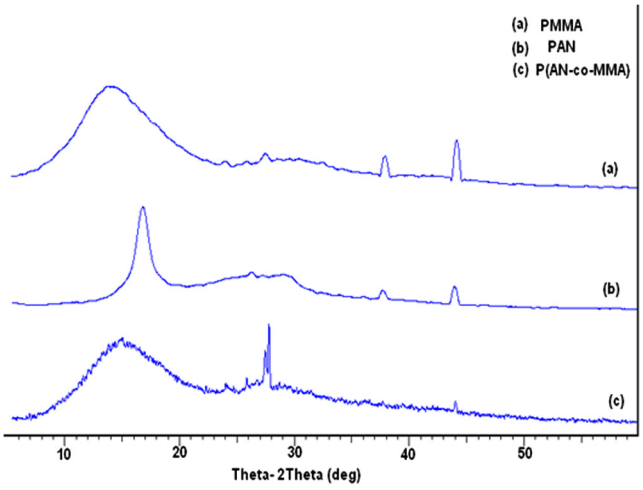

Figure 22 X-ray diffraction patterns of (a) *PMMA*, (b) *PAN* and (c) *P(AN-co-MMA)*.

4. Conclusions

Precipitation polymerization technique has been used in the preparation of poly(AN-Co-MMA) copolymers nanoparticles. The impact of different polymerization conditions on the polymerization conversion yield (PCY) was monitored. It was found that the polymerization conversion yield is linear up to 300 min then tends to slow down with longer polymerization times. At polymerization' temperature below 45 °C, PCY was found to be very low. Linear increment from 10% to 65% was observed with variation of polymerization' temperature from 45 °C to 70 °C. Increase in the water content in the cosolvent from 20% to 70% exponentially increased the PCY up to 60%. Variation of KPS concentration above 0.01% has no effect on PCY. MMA content over 40% has a significant effect on the PCY. The comonomer concentration as all has a clear determining effect on PCY.

Particles size was controlled by variation of the polymerization conditions. KPS concentration over 0.01% increases the size over 100 nm up to microns. Solvent composition with 40–80% water kept the size of particles below 70 nm. Solvent with any other composition produces copolymer particles with a higher size. Polymerization temperature in the range 35 °C to 60 °C, kept the size of copolymer particles less than 70 nm. Polymerization time over 15 min is recommended to have particles size less than 80 nm. Under all polymerization conditions, the particles were produced with a uniform spherical structure.

The structure and composition variation was verified by FT-IR, TGA and nitrogen content analysis. High PAN content copolymers proved to be more thermally stable.

The presented results recommended the preparation of copolymer particles in the nanoscale without any need for emulsifier or dispersion agents and under very mild polymerization conditions and almost aqueous polymerization solvent with minimum alcohol content.

References

Baines, F.L., Dionisio, S., Billiugham, N.C., Armes, S.P., 1996. Use of block copolymer stabilizers for the dispersion polymerization of styrene in alcoholic media. Macromolecules 29 (9), 3096–3102.

Boguslavsky, L., Baruch, S., Margel, S., 2005. Synthesis and characterization of polyacrylonitrile nanoparticles by dispersion/emulsion polymerization process. Colloid Interface Sci. 289, 71–85.

Cao, L., 2006. Covalent Enzyme Immobilization, in Carrier-bound Immobilized Enzymes: Principles, Application and Design, Wiley-VCH Verlag GmbH & Co. KGaA, Weinheim, FRG. <http://dx.doi.org/10.1002/3527607668.ch3>.

Chaitidou, S., Kotrotsiou, O., Kotti, K., Kammona, O., Bukhari, M., Kiparissides, C., 2008. Precipitation polymerization for the synthesis of nanostructured particles. Mater. Sci. Eng B. 152 (1–3), 55–59.

Cheng, F.-L., Zhang, M.-L., Wang, H., 2005. Fabrication of polypyrrole nanowire and nanotube arrays. Sensors 5 (4–5), 245–249.

Cho, Youngnam, Borgens, Richard Ben, 2012. Polymer and nano-technology applications for repair and reconstruction of the central nervous system. Exp. Neurol. 233 (1), 126–144.

Downey, Jeffrey S., Frank, Randy S., Li, Wen-Hui, Stöver, Harald D.H., 1999. Growth mechanism of poly(divinylbenzene) microspheres in precipitation polymerization. Macromolecules 32, 2838–2844.

Guangzhi, Yang, Chunfeng, Zhu, Lei, Zhang, Hanxun, Qiu, Xianying, Wang, Junhe, Yang, 2011. Synthesis and characterization of polyacrylonitrile microspheres by soapless emulsion polymerization. Adv. Mater. Res. 311–313, 571–575.

Horak, D.K., M.; Turkova, J.; Benes, M, Hydrazide-Functionalized Poly(2-hydroxyethyl methacrylate) Microspheres for Immobilization of Horseradish Peroxidase. Biotechnology Progress, 1999. 15: p. 208 - 215.

Ivanov, I.P., Y.L., 2002. Simultaneous immobilisation of uricase and peroxidase to copolymer of acrylonitrile with acrylamide. Biotechnol. Biotechnol. Equip 16, 104–110.

Lee, Ki-Chang, Lee, Seung-Eun, Choi, Yoo-Jin, 2004. Dispersion polymerization of acrylamide in t-butyl alcohol/water media. Macromol. Res. 12 (2), 213–218.

Lee, Jung-Min, Kang, Shin-Jae, Park, Soo-Jin, 2009. Synthesis of polyacrylonitrile based nanoparticles via aqueous dispersion polymerization. Macromol. Res. 17 (10), 817–820.

Liao, Y.H., Zhou, D.Y., Rao, M.M., Li, W.S., Cai, Z.P., Liang, Y., Tan, C.L., 2009. Self-supported poly(methyl methacrylate-acrylonitrile-vinyl acetate)-based gel electrolyte for lithium ion battery". J. Power Sources 189 (1), 139–144.

Lok, Kar P., Ober, Christopher K., 1985. Particle size control in dispersion polymerization of polystyrene. Can. J. Chem. 63, 209–216.

Margel, S., Bamnolker, Hanna, 1996. Dispersion polymerization of styrene in polar solvents: effect of reaction parameters on microsphere surface and surface properties, size and size distribution and molecular weight. Polym. Sci. Part A: Polym. Chem. 34, 1857.

Mohy Eldin, M.S., Elaassar, M.R., Elzatahry, A.A., Al-Sabah, M.M.B., Hassan, E.A., 2012. Covalent immobilization of β-galactosidase onto amino-functionalized PVC microspheres. Appl. Polym. Sci. 125 (3), 1724–1735.

Paine, Anthony James, Lumes, Wayne, McNulty, James, 1990. Dispersion polymerization of styrene in polar solvents. 6. Influence of reaction parameters on particle size and molecular weight in poly(N-vinylpyrrolidone)-stabilized reactions. Macromolecules 23 (12), 3104–3109.

Rajendran, S., Sivakumar, M., Subadevi, R., 2003. Effect of salt concentration in poly(vinyl alcohol)-based solid polymer electrolytes. Power Sources 124 (1), 225–230.

Rao, M.M., Liu, J.S., Li, W.S., Liang, Y., Liao, Y.H., Zhao, L.Z., 2008. Performance improvement of poly(acrylonitrile-vinyl acetate) by activation of poly(methyl methacrylate). J. Power Sources.

Sáenz, José M., Asua, José M., 1998. Kinetics of the dispersion copolymerization of styrene and butyl acrylate. Macromolecules 31 (16), 5215–5222.

Shen, S., Sudol, E.D., El-Aasser, M.S., 1994. Dispersion polymerization of methyl methacrylate: mechanism of particle formation. Polym. Sci. Part B: Polym. Chem. 32 (6), 1087–1100.

Shi, S., Kuroda, S., Hosoi, K., Kubota, H., 2005. Poly(methyl methacrylate)/polyacrylonitrile composite latex particles with a novel surface morphology. Polymer 46, 3567–3570.

Tanrisever, T., Okay, O., Sonmezoglu, I.C., 1996. Kinetics of emulsifier-free emulsion polymerization of methyl methacrylate. Appl. Polym. Sci. 61 (3), 485–493.

Thapa, A., Webster, T.J., Haberstroh, K.M., 2003. Polymers with nano-dimensional surface features enhance bladder smooth muscle cell adhesion. J. Biomed. Mater. Res. 67A, 1374–1383.

Tuncel, A., 2000. Emulsion copolymerization of styrene and poly(ethylene glycol) ethyl ether methacrylate. Polymer 41 (4), 1257–1267.

Wei, S., Molinelli, A., Mizaikoff, B., 2006. Molecularly imprinted micro and nanospheres for the selective recognition of 17β-estradiol. Biosens. Bioelectron. 21, 1943–1951.

Yang, Y., Chu, Y., Yang, F., Zhang, Y., 2005. Uniform hollow conductive polymer microspheres synthesized with the sulfonated polystyrene template. Mater. Chem. Phys. 92 (1), 164–171.

Ye, L., Cormack, P.A.G., Mosbach, K., 1999. Molecularly imprinted monodisperse microspheres for competitive radioassay. Anal. Commun. 36, 35–38.

Zhang, L., Zhang, S.-C., 2007. Preparation and characterization of poly(acrylonitrile-co-methoxy polyethylene glycol monoacrylat-co-lithiumacrylate). Acta Phys. Chim. Sin. 23, 1943–1947.

Zhang, H.P., Zhang, P., Li, Z.H., Sun, M., Wu, Y.P., Wu, H.Q., 2007a. A novel sandwiched membrane as polymer electrolyte for lithium ion battery. Electrochem. Commun. 9 (7), 1700–1703.

Zhang, S.P., Fu, X.K., Gong, Y.F., 2007b. Spectroscopic and electrochemical studies on block-polymer/PMMA blend based composite polymer electrolytes. Appl. Polym. Sci. 106 (6), 4091–4097.

Zhang, Hong-Tao, Yuan, Xiao-Ya, Huang, Jin-Xia, 2004. Study of kinetics and nucleation mechanism of dispersion copolymerization of methyl methacrylate and acrylic acid. React. Funct. Polym. 59 (1), 23–31.

Zhou, D.Y., Wang, G.Z., Li, W.S., Li, G.L., Tan, C.L., Rao, M.M., Liao, Y.H., 2008. Preparation and performances of porous polyacrylonitrile–methyl methacrylate membrane for lithium-ion batteries. J. Power Sources 184, 477–480.